

VERTICAL BEAM SIZE MEASUREMENT METHODS AT THE BESSY II STORAGE RING AND THEIR RESOLUTION LIMITS

M. Koopmans*^{†1}, F. Armborst^{†1}, J.-G. Hwang, A. Jankowiak¹, P. Kuske, M. Ries, G. Schiwietz
Helmholtz-Zentrum Berlin für Materialien und Energie GmbH (HZB), Berlin, Germany
¹also at Humboldt-Universität zu Berlin, Berlin, Germany

Abstract

With the VSR upgrade for the BESSY II electron storage ring bunch resolved diagnostics are required for machine commissioning and to ensure the long-term quality and stability of operation. For transverse beam size measurements we are going to use an interferometric method, which will be combined with a fast gated intensified CCD camera at a subsequent stage. A double-slit interferometer method has already been verified successfully at BESSY II. In addition first 2D bunch resolved measurement tests have been performed at the dedicated diagnostics beamline for bunch length measurements. Measurements of the interferometer and X-ray pinholes as a function of a vertical electron beam excitation are compared in this paper.

INTRODUCTION

The upgrade project of the BESSY II storage ring towards the variable pulse length storage ring BESSY VSR relies on intense short pulses as well as high average photon flux simultaneously [1, 2]. The filling pattern will feature bunches varying in length, current, and charge density over an order of magnitude. This variation will also cause different transverse beam sizes for the various bunch types. Therefore non-invasive bunch resolved diagnostics are needed for the commissioning and development of BESSY VSR providing long term quality and stability of user operation. Dedicated diagnostic beamlines are under development [3].

The transverse beam size is monitored with two pinhole systems [4] at BESSY II. In addition an interferometric beam size monitor (IBSM) has been set up and successfully commissioned for various applications [5, 6]. These systems are not able to measure bunch resolved beam sizes yet, but it is planned to move the IBSM to the new VSR diagnostics beamline and upgrade the system applying gating techniques, e. g. with an ICCD camera, which then allows bunch resolved measurements [3]. In contrast to the IBSM, the pinhole systems cannot be upgraded easily to provide bunch resolved information, since they are based on a slow conversion process of X-rays into visible light.

This paper focuses on comparing the beam sizes measured with the pinhole systems and the IBSM for a variable source size. These measurements are combined with data from beam loss monitors. Using the loss rate as another beam size dependent parameter, the resolution limit of different systems can be extracted. In addition first results towards

2D bunch resolved measurements at the new VSR beamline dedicated for bunch length measurements are shown.

TRANSVERSE BEAM SIZE MEASUREMENTS

Measurement Systems

The two pinhole systems (PINH3, PINH9) use direct imaging with X-rays, with a mean energy of 16.33 keV to measure the beam size. The X-rays are then converted to visible light by a phosphor screen and imaged onto a CCD camera [4].

The Interferometer uses synchrotron radiation (SR) in the visible range from a bending magnet. The light is diffracted by a double slit and is then imaged onto a CCD camera using a bandpass and a polarisation filter. The interference pattern on the detector plane can be described with [7]:

$$I(x) = I_0 \operatorname{sinc}^2 \left(\frac{\pi a}{\lambda f} x \right) \left[1 + V \cos \left(\frac{2\pi d}{\lambda f} x + \psi \right) \right], \quad (1)$$

where x is the position at the detector, a the full single slit width, d the full slit distance, f the distance between the lens and the detector surface, λ the wavelength, ψ the relative photon phase, I_0 the intensity at the slits and V the so called visibility. Given the distance L to the source and assuming Gaussian beams and equal intensity at both slits, the beam size can be obtained from the fitted visibility via [6, 7]

$$\sigma_x = \frac{\lambda L}{\pi d} \sqrt{\frac{1}{2} \ln \left(\frac{1}{V} \right)}. \quad (2)$$

Vertical Beam Size Measurement

The performance of the systems is tested by measuring the beam size over a larger range. We will only consider measurements in vertical direction, since it is easier to manipulate the beam size in the vertical direction. At the BESSY II storage ring the vertical beam size can be varied by applying a vertical excitation U with a broadband noise signal [6].

The measurement of the vertical beam size with both pinhole systems and the interferometer as a function of the excitation is shown in Fig. 1. The measurement was done in standard user optics with 250 mA beam current.

While the IBSM measures the widest range of beam sizes, all three systems produce different measurements and behave differently when varying the beam size. These differences cannot be explained with the differences of the twiss parameters [8] at the source point, since they are similar for all three systems, and imply different resolution limits for each system.

* marten.koopmans@helmholtz-berlin.de

[†] Doctoral researcher at Humboldt-Universität zu Berlin

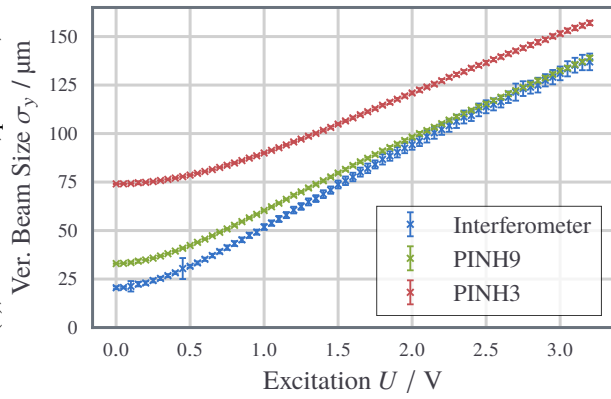


Figure 1: Measured vertical beam size by the pinhole systems and the interferometer as a function of the vertical excitation.

RESOLUTION OF SYSTEMS

For small excitations the vertical beam size is expected to have the following dependence on the excitation:

$$\sigma_{\text{model}}^2(U) = \sigma_0^2 + \alpha^2 U^2, \quad (3)$$

with a beam size at zero excitation σ_0 and a linear coupling α . The problem is however, that the systems have a (different) resolution which is not considered in Eq. 3. Adding an additional term σ_{res} for the resolution to Eq. 3 describes the beam size which is actually measured

$$\sigma_{\text{meas}}^2(U) = \sigma_{\text{res}}^2 + \sigma_{\text{model}}^2(U) = \sigma_{\text{res}}^2 + \sigma_0^2 + \alpha^2 U^2. \quad (4)$$

So the measurements in Fig. 1 show a combination of the resolution and the true beam size, which cannot be distinguished by a single system or multiple systems with similar resolution limits.

The idea was then to combine the measurements with an additional parameter. A possible parameter for storage rings is the lifetime. However, the lifetime cannot be measured directly. Therefore the loss rate was chosen, which is monitored very accurately at different positions around the ring and is inversely proportional to the lifetime.

Beam Loss Monitors

The beam loss monitors are based on sodium iodide scintillation counters and are installed in high dispersion regions, sensitive for Touschek losses [9].

The measured loss rate R is composed by a beam size dependent and a beam size independent term:

$$R = R_{\text{const}} + R_{\sigma}. \quad (5)$$

The constant term R_{const} is expected not to change with the shape of the beam, only depending on the vacuum conditions and the beam current. The beam size dependent term R_{σ} is caused by the Touschek effect related to the repulsive electron-electron interaction. The loss rate caused by Touschek effect is proportional to the current density and therefore scales inversely to the volume of the beam. Hence, for a manipulation of the beam in a single dimension, that this term is inversely proportional to the vertical beam size $R_{\sigma} \propto \sigma^{-1}$. Using this and the model from Eq. 3 the inverse

loss rate is then given by:

$$R = R_{\text{const}} + \frac{\xi}{\sqrt{\sigma_0^2 + \alpha^2 U^2}} = R_{\text{const}} + \frac{1}{\sqrt{a^2 + b^2 U^2}}, \quad (6)$$

with the constants $a = \sigma_0/\xi$ and $b = \alpha/\xi$.

The measured loss rate is shown as a function of the vertical excitation in Fig. 2. Here the measurements of four beam loss monitors, BLM1 to BLM4, are used which are located between the achromatic bends where the dispersion reaches its maximum.

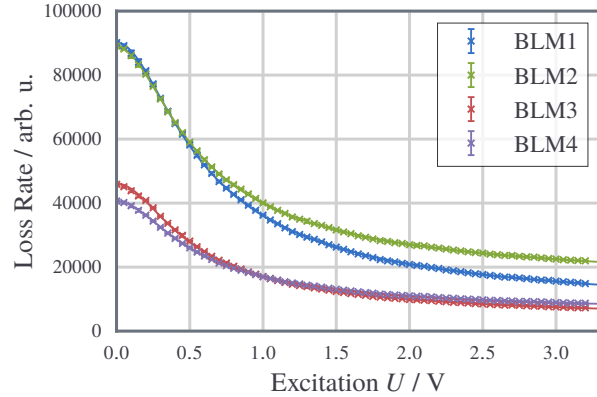


Figure 2: Loss rate measured by four beam loss monitors as a function of the vertical excitation. The data is fitted according to Eq. (6).

Before comparing the loss rates with the beam sizes it is necessary to eliminate the beam size independent contribution to the loss rate to obtain the beam size dependent loss rate, which will be defined as corrected loss rate. Therefore the loss rates are fitted with Eq. 6. The fits can be seen together with the measured loss rates in Fig. 2. With the obtained constants the beam size independent loss rate is subtracted from the measured loss rate. The corrected loss rates are then normalized and the inverse loss rates are shown in Fig. 3.

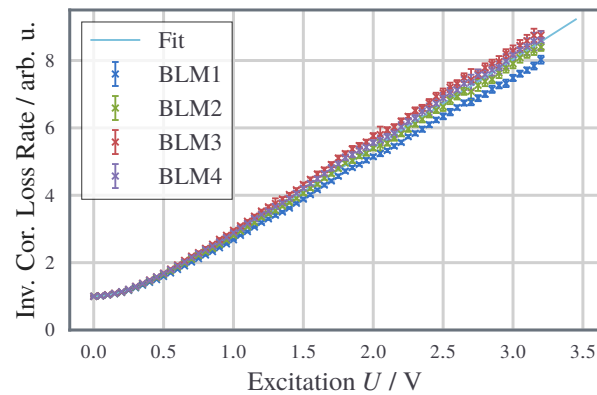


Figure 3: Inverse corrected loss rate of the four different beam loss monitors as a function of the vertical excitation. The fit shows the average result.

The corrected and rescaled loss rates are similar for the four different loss monitors. For further analysis the average

of the inverse normalized corrected loss rate is used, which is also shown by the fit in Fig. 3.

Combination

Now it is possible to describe the beam size as a function of the inverse loss rate instead of the excitation. The extrapolated value at $1/R_{\text{cor}} = 0$ is equal to σ_{res} and the lowest measured value corresponds to $\sqrt{\sigma_{\text{res}}^2 + \sigma_0^2}$, implying

$$\sigma_0^2 = \sigma_{\text{meas}}^2(U=0) - \sigma_{\text{res}}^2. \quad (7)$$

The vertical beam size as a function of the average inverse corrected loss rate is shown in Fig. 4 together with the corresponding fits. The fit is performed only for small excitations ($U < 1.5$ V). The results are summarized in Table 1.

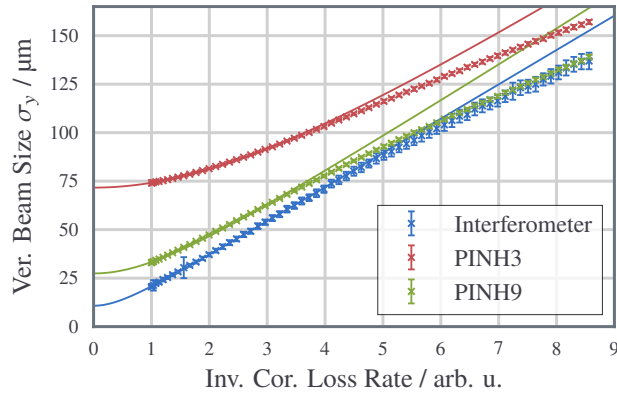


Figure 4: Measured vertical beam size as a function of the inverse corrected loss rate. The fit uses only data for small excitations below 1.5 V.

Table 1: Results for σ_{res} and σ_0 from the Fits Shown in Fig. 4

System	$\sigma_{\text{res}} / \mu\text{m}$	$\sigma_0 / \mu\text{m}$
Interferometer	10.8 ± 0.2	17.77 ± 0.04
PINH3	71.67 ± 0.05	19.1 ± 0.1
PINH9	27.4 ± 0.2	18.9 ± 0.1

All three systems give a similar beam size for no excitation of about $18 \mu\text{m}$ to $19 \mu\text{m}$. The resolutions however differ significantly. In the used configuration the IBSM has a resolution of $10.8 \mu\text{m}$. The resolution of PINH9 is $27.4 \mu\text{m}$ and the resolution of PINH3 is over $70 \mu\text{m}$. The stated uncertainties include only the corresponding statistical error. Using the lattice model, these measurements correspond to an average vertical emittance of 16 pm rad at no excitation and to 130 pm rad in standard user operation, where the excitation is set to 1 V.

OUTLOOK – 2D-DIAGNOSTICS

At the new VSR diagnostics beamline dedicated for bunch length measurements first tests were performed to show the feasibility of two dimensional bunch resolved measurements. The measurements were done with a HAMAMATSU streak camera C10910. The beam was rotated by 90° , so that the

horizontal profile of the beam on the streak camera corresponds to the vertical beam size. The tests were also done with the vertical excitation. The streak camera measurement for zero and 5 V excitation with π -polarisation is shown in Fig. 5. In addition, the horizontal projection for the center of the bunches is shown. The averaged horizontal intensity projection of the bunches in Fig. 5 is also shown for different excitations in 1 V steps in Fig. 6.

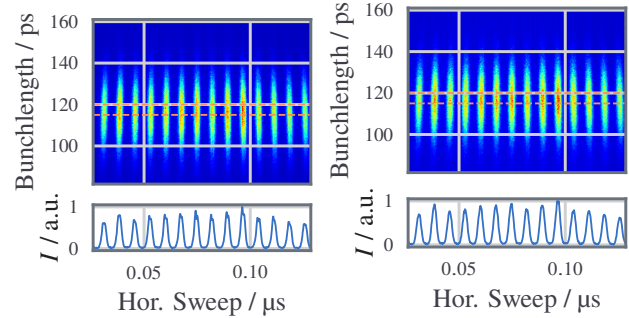


Figure 5: Streak camera images with π -polarisation taken at zero (left) and 5 V (right) excitation and the intensity projection for the bunch center (dashed red line).

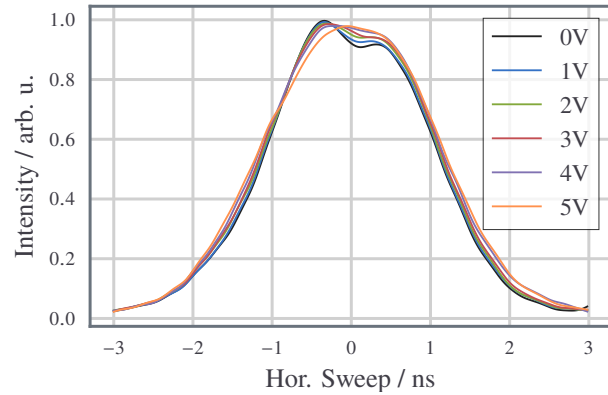


Figure 6: Averaged horizontal intensity projections of the bunch centers for excitations from 0 V to 5 V.

The streak camera images show that the setup is sensitive to the vertical beam size. The characteristic dip in the center of π -polarized SR is vanishing for larger beam sizes. However, these are only first qualitative results and the setup will be improved. Moreover, a quantitative analysis as in [10] using full beamline simulation is planned.

CONCLUSION

Measurements with the pinhole systems and the IBSM were done and compared for a variable vertical beam size. The resolution of the systems and the true beam size were obtained using the loss rate. In addition first qualitative 2D bunch resolved results are observed, providing a variety of advanced diagnostic options for the VSR project.

REFERENCES

- [1] A. Jankowiak *et al.*, eds., “BESSY VSR – Technical Design Study”, Helmholtz-Zentrum Berlin für Materialien und Energie GmbH, Germany, June 2015. doi:10.5442/R0001
- [2] P. Schnizer *et al.*, “Status of the BESSY VSR Project”, in *Proc. IPAC’18*, Vancouver, Canada, Apr.-May 2018, pp. 4138–4141. doi:10.18429/JACoW-IPAC2018-THPMF038
- [3] G. Schiwietz *et al.*, “Development of the Electron-Beam Diagnostics for the Future BESSY-VSR Storage Ring”, in *Proc. IPAC’18*, Vancouver, Canada, Apr.-May 2018, pp. 2110–2113. doi:10.18429/JACoW-IPAC2018-WEPAK011
- [4] K. Holldack *et al.*, “Source size and emittance monitoring on BESSY II”, *Nucl. Instr. Meth. A*, vol. 467–468, pp. 235–238, 2001. doi:10.1016/S0168-9002(01)00555-1
- [5] M. Koopmans *et al.*, “Status of a Double Slit Interferometer for Transverse Beam Size Measurements at BESSY II”, in *Proc. IPAC’17*, Copenhagen, Denmark, May 2017, pp. 149–152. doi:10.18429/JACoW-IPAC2017-MOPAB032
- [6] M. Koopmans, “Interferometric Beam Size Monitor for BESSY II”, Master thesis, Humboldt-Universität zu Berlin, Berlin, Germany, 2017.
- [7] T. Mitsuhashi, “Beam Profile and Size Measurement by SR Interferometer”, *Beam measurement*, Ed. by S. Kurokawa *et al.*, pp. 399–427, World Scientific 1999.
- [8] H. Wiedemann, *Particle Accelerator Physics*, 3rd ed. Berlin, Germany: Springer, 2007.
- [9] P. Kuske, “Accelerator Physics Experiments with Beam Loss Monitors at BESSY”, in *Proc. DIPAC’01*, Grenoble, France, May 2001, paper IT07, pp. 31–35.
- [10] J. Breunlin *et al.*, “Methods for measuring sub-pm rad vertical emittance at the Swiss Light Source”, in *Nucl. Instrum. Meth. A*, vol. 803, pp. 55-64, 2015.